Short communication

Lithium-ion batteries modeling involving fractional differentiation

Jocelyn Sabatier [a,*], Mathieu Merveillaut [a], Junior Mbala Francisco [b], Franck Guillemard [b], Denis Porcelatto [b]

[a] IMS, UMR 5218 CNRS, 351 cours de la Libération, 33405 Talence Cedex, France
[b] PSA Peugeot Citroën, 2, route de Gisy, 78943 Velizy-Villacoublay Cedex, France

HIGHLIGHTS

- A simplified model is obtained from a lithium-ion battery electrochemical model.
- Fractional differentiation is used for a low number of parameters in the model.
- Some electrochemical variables and parameters still appear in the simplified model.
- A relative error less than 0.5% on the voltage is obtained under various conditions.
- The model simplicity and the accuracy are interesting for use in automobile BMS.

ARTICLE INFO

ABSTRACT

With hybrid and electric vehicles development, automobile battery monitoring systems (BMS) have to meet the new requirements. These systems have to give information on state of health, state of charge, available power. To get this information, BMS often implement battery models. Accuracy of the information manipulated by the BMS thus depends on the model accuracy. This paper is within this framework and addresses lithium-ion battery modeling. The proposed fractional model is based on simplifications of an electrochemical model and on resolution of some partial differential equations used in its description. Such an approach permits to get a simple model in which electrochemical variables and parameters still appear.

1. Introduction

More and more drastic automobile pollution norms and oil price increase, lead car manufacturers to design new vehicles (stop and start, hybrid, or electric). The underlying idea is to reduce exhaust emissions in the built-up areas, either by stopping the internal combustion engine when the vehicle is not moving, or by substituting electric fuel for fossil fuel. The latter may involve an electric motor and one or more energy storage system. To keep these new vehicles in good working order, car manufacturers must integrate a reliable electrical energy storage management [1]. That is why, state of charge (SOC) and state of health (SOH) estimators must be designed. To design these estimators, dynamical models of the battery pack can be a valuable tool.

In this paper, a dynamical model of a lithium-ion battery is proposed. Many models exist in the literature for this kind of batteries such as purely electric models [2] or fuzzy models [3]. An extensive analysis on lithium ion batteries modeling in proposed in Ref. [4]. The originality here is the way this model is obtained. It results from simplification of an electrochemical model that describes the battery behavior using partial differential equations. Interest of this approach is that it is possible to link the electrochemical parameters of the battery to the resulting dynamic model parameters. This model has thus an important physical meaning, unlike purely electric models proposed in the literature. Another interest is the introduction of fractional differentiation that helps to describe some parts of the model with a small number of parameters again directly related to the electrochemical parameters of the battery. As shown on several electrochemical devices [5–8], fractional differentiation permits to obtain models with a low number of parameters. Such a model can thus be used for SOC or SOH estimator design.

* Corresponding author. Tel.: +33 5 40 00 83 01; fax: +33 5 40 00 83 44.
E-mail address: Jocelyn.sabatier@ims-bordeaux.fr (J. Sabatier).

2. Electrochemical model

The simplified model that will be presented in the sequel is based on lithium-ion electrochemical presented in Refs. [9,10] that results in Newman's modeling approach [11]. This model is a pseudo 2D based on a representation of the cell such as in Fig. 1.

In Fig. 1, the electrodes are seen as an aggregation of spherical particles (2D representation) in which the Li$^+$ ions are inserted. The first spatial dimension of this model, represented by variable x, is the horizontal axis. The second spatial dimension is the particle radius.

The cell is constituted of three regions (two electrodes and a separator) that imply four distinct boundaries at:

- $x = 0$: negative electrode current collector;
- $x \in]0; \delta_n[$: region 1, δ_n thickness negative carbon electrode (Li$_x$C$_6$, MCMB···);
- $x = \delta_n$: negative electrode/separator interface;
- $x \in]\delta_n ; \delta_n + \delta_{sep}[$: region 2, δ_{sep} thickness separator;
- $x = \delta_n + \delta_{sep}$: separator/positive electrode interface;
- $x \in]\delta_n + \delta_{sep} ; L[$: region 3, δ_p thickness positive electrode made of LiCoO$_2$;
- $x = L$: positive electrode current collector.

The two electrodes are assumed electrochemically porous. Regions 1 and 3 are therefore constituted of a solid phase (electrode material) and a liquid phase (electrolyte).

The cell is supposed supplied by a current $I(t)$. The cell voltage denoted $U_{batt}(t)$ is defined by the relation

$$U_{batt}(t) = \phi_s(L, t) - \phi_s(0, t) - \frac{R_f}{A} I(t) \qquad (1)$$

where $\varphi_s(L,t)$ and $\varphi_s(0,t)$ are respectively the positive electrode potential at abscissa $x = L$ and the negative electrode potential at abscissa $x = 0$; R_f denotes the contact resistance and A the electrodes surface. Note that all the parameters used in the following equations are defined in Refs. [9,10].
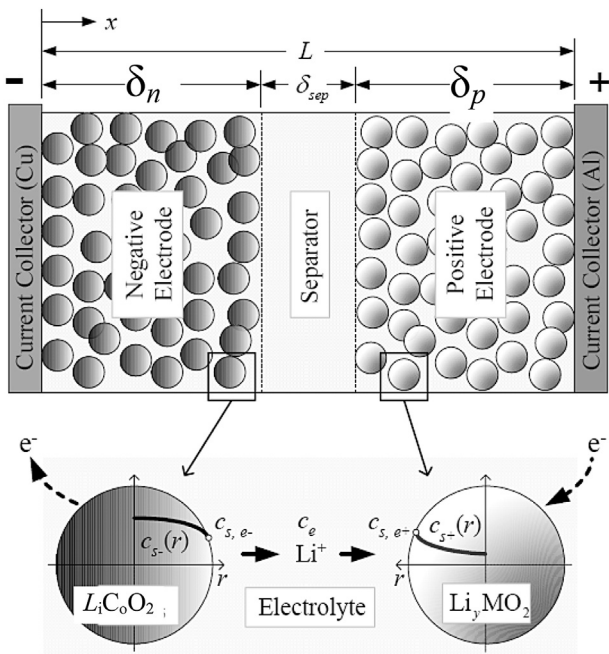

Fig. 1. Pseudo 2D model of a lithium-ion cell [9,10].

As described in Refs. [9,10], lithium concentration $c_s(x, r, t)$ evolution in the spherical particle of radius $r = R_s$, is supposed described by the diffusion law,

$$\frac{\partial c_s}{\partial t} = \frac{D_s}{r^2} \frac{\partial}{\partial r} \left(r^2 \frac{\partial c_s}{\partial r} \right) \quad \begin{cases} \left. \dfrac{\partial c_s}{\partial r} \right|_{r=0} = 0 \\[2mm] \left. D_s \dfrac{\partial c_s}{\partial r} \right|_{r=R_s} = \dfrac{-j^{Li}}{a_s F} \end{cases} \qquad (2)$$

Lithium concentration $c_e(x, t)$ in the electrolyte is modeled by:

$$\frac{\partial(\varepsilon_e c_e)}{\partial t} = \frac{\partial}{\partial x} \left(D_e^{eff} \frac{\partial}{\partial x} c_e \right) + \frac{1 - t_+^o}{F} j^{Li}, \qquad (3)$$

with

$$\left. \frac{\partial c_e}{\partial x} \right|_{x=0} = \left. \frac{\partial c_e}{\partial x} \right|_{x=L} = 0. \qquad (4)$$

Charge conservation in the solid phase of each electrode is defined by the Ohm's law:

$$\frac{\partial}{\partial x} \left(\sigma^{eff} \frac{\partial}{\partial x} \phi_s \right) - j^{Li} = 0, \qquad (5)$$

with the following limit conditions at the current collectors

$$-\sigma_-^{eff} \left. \frac{\partial \phi_s}{\partial x} \right|_{x=0} = \sigma_+^{eff} \left. \frac{\partial \phi_s}{\partial x} \right|_{x=L} = \frac{I}{A}, \qquad (6)$$

and the null current conditions at the separator:

$$\left. \frac{\partial \phi_s}{\partial x} \right|_{x=\delta_n} = \left. \frac{\partial \phi_s}{\partial x} \right|_{x=\delta_n + \delta_{sep}} = 0. \qquad (7)$$

If $\phi_e(x, t)$ denotes the electrolyte potential, charge conservation in the electrolyte is defined by:

$$\frac{\partial}{\partial x} \left(\kappa^{eff} \frac{\partial}{\partial x} \phi_e \right) + \frac{\partial}{\partial x} \left(\kappa_D^{eff} \frac{\partial}{\partial x} \ln(c_e) \right) + j^{Li} = 0, \qquad (8)$$

with the limit conditions

$$\left. \frac{\partial \phi_e}{\partial x} \right|_{x=0} = \left. \frac{\partial \phi_e}{\partial x} \right|_{x=L} = 0. \qquad (9)$$

The four differential equations (2), (3), (5) and (8) that describe variables $c_{s,e}, c_e, \phi_s, \phi_e$, variations are linked by the Butler–Volmer equation

$$j^{Li} = a_s i_o \left\{ \exp \left[\frac{\alpha_a F}{RT} \eta \right] - \exp \left[-\frac{\alpha_c F}{RT} \eta \right] \right\}. \qquad (10)$$

In equation (10), j^{Li} is induced by overvoltage η, defined by the potential difference between the solid phase and the electrolyte and equilibrium thermodynamic potential U:

$$\eta = \phi_s - \phi_e - U. \qquad (11)$$

The equilibrium potential U is a function of the solid phase concentration at the spherical particles. System input is the current $I(t)$ in equation (6). System output is the cell voltage given by equation (1).

3. From the electrochemical model to a fractional dynamic model

The approach is here to reduce the electrochemical model equations (1)–(11) to simpler equations taking into account simplifying assumptions and using some approximations. This kind of approach has been recently used in Ref. [12] that supposes small signal current or potential as excitations applied to the battery. These excitations permit to simplify the electrochemical model and to extract battery impedance. Here small signal current or potential as excitations are not used. The electrochemical model previously described has been implemented under Comsol Multiphysics and its parameters have been adjusted to fit a SAFT VL7P battery behavior. This model is then used to speculate assumptions and approximations that are now presented, and then to propose a simplified model. The assumptions introduced are formally proved and the approximation used will then be validated through the simplified model accuracy.

3.1. Assumptions

• Assumption H_1

Due to the low resistivity of electrode materials, it is supposed that the solid phase potentials are constants in the two electrodes:

$$\phi_s(x,t) = \phi_{s\_moy}(t). \tag{12}$$

Moreover, negative electrode is supposed connected to the ground. Negative electrode solid phase potential is thus null:

$$\phi_{sn}(t) = \phi_s(x,t) = \phi_{s\_moy}(t) = 0 \quad \forall x \in [0, \delta_n]. \tag{13}$$

To illustrate assumption H_1 validity, the current profile of Fig. 2 is applied to the electrochemical model. The resulting potentials are represented by Fig. 3a.
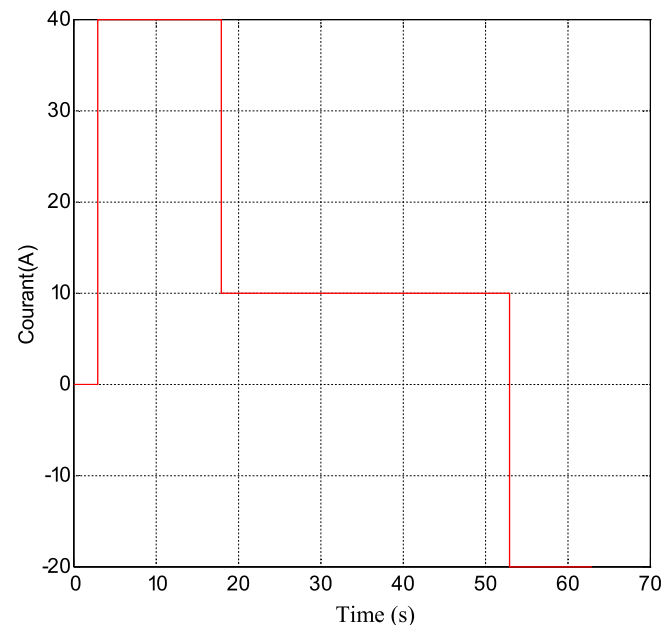
• Approximation A_1

Fig. 2. Current profile used to validate assumption H_1.

It is supposed that electrolyte potentials are constants in the two electrodes. It is moreover supposed equal to its mean value for a given electrode:

$$\phi_e(x,t) = \phi_{e\_moy}(t). \tag{14}$$

For current in Fig. 2, Fig. 3b shows the electrolyte potentials in the electrodes and in the separator. It permits to assess approximation A_1 quality and to check that this potential remains close to 0.6 V.

• Approximation A_2

Current density j^{Li} is supposed constant in each electrode. It is moreover supposed equal to its mean value for a given electrode:

$$j_i^{Li}(t) = j_{i\_mean}^{Li}(t) \overset{\Delta}{=} \frac{1}{\delta_i} \int_0^{\delta_i} j^{Li}(t,x) dx \tag{15}$$

with $i = n,p$ (n = negative electrode, p = positive electrode).

For current in Fig. 2, Fig. 4 shows the current density $j^{Li}(t)$ in the 2 electrodes and permits to assess approximation A_2 quality for the positive electrode. Due to the low impact of the negative electrode on the whole cell behavior (this electrode only create small voltage variations, aging been not modeled here), assumption A_2 is also adopted for this electrode.

Equation (5) integration for negative electrode leads to:

$$\sigma_{eff}\left[\left(\frac{\partial}{\partial x}\phi_s(t,x)\right)\bigg|_{x=\delta_n} - \left(\frac{\partial}{\partial x}\phi_s(t,x)\right)\bigg|_{x=0}\right] = \int_0^{\delta_n} j_n^{Li}(t,x) dx \tag{16}$$

or given equations (6) and (7)

$$\frac{I(t)}{A} = \int_0^{\delta_n} j_n^{Li}(t,x) dx \tag{17}$$

and thus given approximation A_2 and for the two electrodes

$$j_{i\_mean}^{Li}(t) = \frac{I(t)}{A\delta_i} = j_i^{Li}(t) \quad i = n,p. \tag{18}$$

• Assumption H_2

Butler–Volmer equation defined by

$$j_{i\_mean}^{Li}(t) = a_{si}i_{0i}\left\{\exp\left(\frac{\alpha_a F}{RT}\eta_i(t)\right) - \exp\left(-\frac{\alpha_c F}{RT}\eta_i(t)\right)\right\}, \tag{19}$$

with

$$\eta_i(t) = \phi_{si}(t) - \phi_{ei}(t) - U_i(t) \tag{20}$$

is supposed linear on the current range defined by table in Fig. 5 for a SAFT VL7P battery.

This assumption is now formally validated using the electrochemical model reminded in section 2. Even with a high value current (a positive strobe followed by a negative one with 100 A each), η_i variations remains close to 0 (see Fig. 6).

Using the first term of the Taylor expansion of the exponential function in equation (19), a linear approximation of this relation is thus:
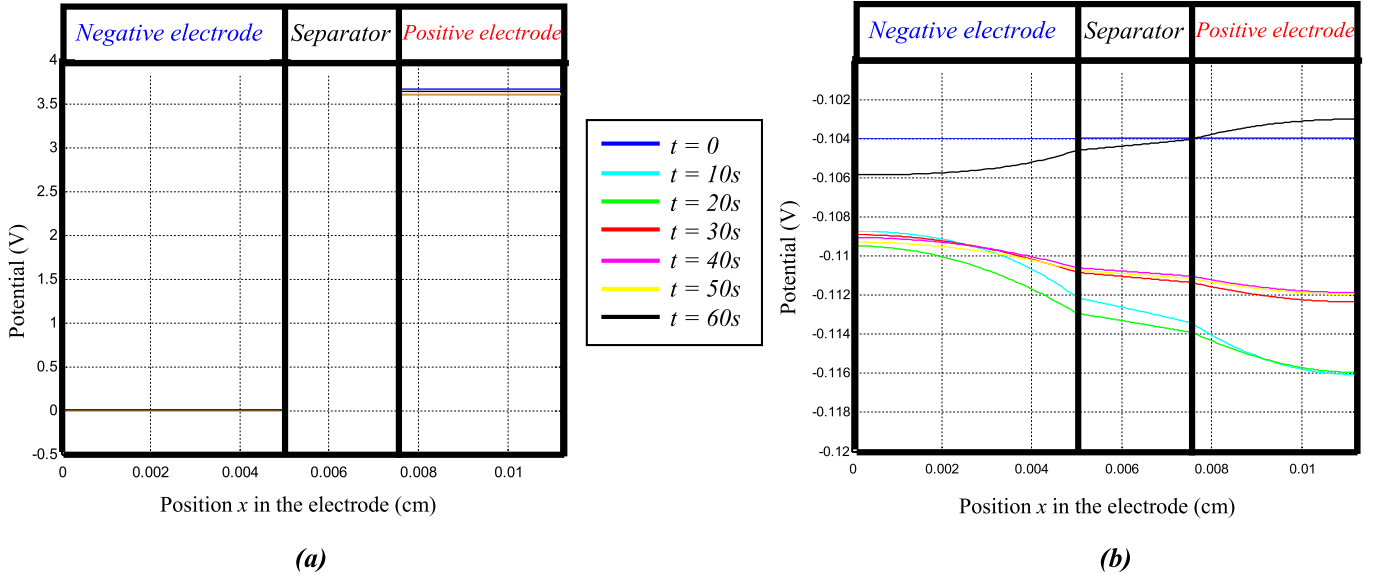
Fig. 3. Solid phase (a) and electrolyte (b) potential in all the cell.

$$j_{i\_\text{mean}}^{\text{Li}}(t) = a_{si}i_{0i}\left(\frac{\alpha_a F}{RT}\eta_i(t) + \frac{\alpha_c F}{RT}\eta_i(t)\right) \quad (21)$$

with $\alpha_a + \alpha_c = 1$. Using only a graph, it is then easy to check that this approximation leads to an error less then 0.2% for supply currents close to 250 A (maximal peak current).

Using equations (19) and (20), then:

$$\phi_{ei}(t) = \phi_{si}(t) - U_i(t) - \frac{j_{i\_\text{mean}}^{\text{Li}}}{\frac{a_{si}i_{0i}F}{RT}(\alpha_a + \alpha_c)}. \quad (22)$$

- Assumption H_3

Lithium concentration in the separator is supposed a linear function of x around the initial value denoted $C_{ei}(x,0)$. As in the separator J^{Li} is null, Laplace transform of equation (3) is:
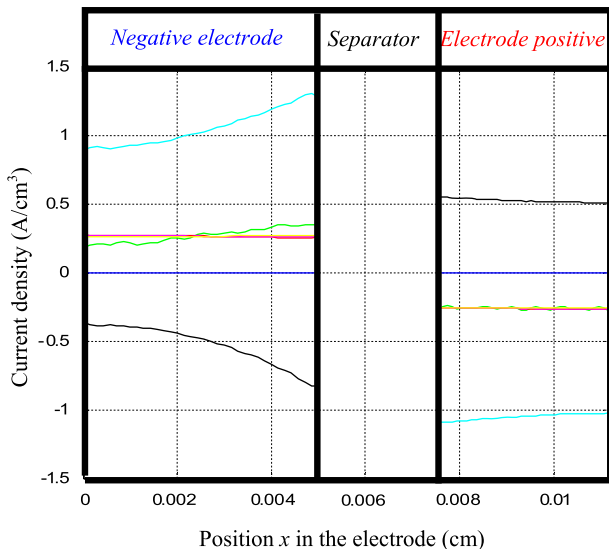
Fig. 4. Current density j^{Li} in the electrodes.

$$\varepsilon_e(C_e(x,p) - C_e(x,0)) = \frac{\partial}{\partial x}\left(D_e^{\text{eff}}\frac{\partial}{\partial x}C_e(x,p)\right) \quad (23)$$

or if D_e^{eff} and ε_e are supposed constant as in Ref. [10],

$$C_e(x,p) - C_e(x,0) = \frac{D_e^{\text{eff}}}{\varepsilon_e}\frac{\partial^2}{\partial x^2}C_e(x,p). \quad (24)$$

A solution of equation (24) is

$$C_e(x,p) = e^{\frac{x\sqrt{\varepsilon_e}}{\sqrt{D_e^{\text{eff}}}}}C_1 + e^{\frac{-x\sqrt{\varepsilon_e}}{\sqrt{D_e^{\text{eff}}}}}C_2 + C_e(x,0) \quad (25)$$

in which C_1 and C_2 are two constants depending on limit conditions. As $x\sqrt{\varepsilon_e}/\sqrt{D_e^{\text{eff}}}$ is a small quantity, then $e^{x\sqrt{\varepsilon_e}/\sqrt{D_e^{\text{eff}}}} \approx 1 + x\sqrt{\varepsilon_e}/\sqrt{D_e^{\text{eff}}}$ and equation (25) becomes

$$C_e(x,p) \approx \frac{x\sqrt{\varepsilon_e}}{\sqrt{D_e^{\text{eff}}}}(C_1 - C_2) + C_1 + C_2 + C_e(x,0) \quad (26)$$

which is the equation of a straight line if $C_e(x,0)$ is constant or also a straight line. This thus validates assumption H_3.

This assumption validity is also illustrated by Fig. 7.

In the separator, equation (8) becomes

$$\frac{\partial}{\partial x}\left(\kappa^{\text{eff}}\frac{\partial}{\partial x}\phi_{ei}(x,t)\right) + \frac{\partial}{\partial x}\left(\frac{\kappa_D^{\text{eff}}}{c_{ei}(x,t)}\frac{\partial}{\partial x}c_{ei}(x,t)\right) = 0, \quad (27)$$

or after integration,

$$\kappa^{\text{eff}}\frac{\partial}{\partial x}\phi_{ei}(x,t) + \frac{\kappa_D^{\text{eff}}}{c_{ei}(x,t)}\frac{\partial}{\partial x}c_{ei}(x,t) = C. \quad (28)$$

Limit conditions (9) shows that constant C is equal to 0, and thus equation (28) becomes

$$\kappa^{\text{eff}}\frac{\partial}{\partial x}\phi_{ei}(x,t) + K_{ce}\kappa_D^{\text{eff}}\frac{\partial}{\partial x}c_{ei}(x,t) = 0 \quad (29)$$

with $K_{ce} = 1/c_{ei}(x,0)$.

	VL7 P	VL20 P	VL30 P
Electrical characteristics			
Nominal voltage (V)	3,6	3,6	3,6
Average capacity 1C after charge to 4.0 V/cell (Ah)	7	20	30
Minimum capacity 1C after charge to 4.0 V/cell (Ah)	6,5	18,5	28
Specific energy after charge to 4.0 V/cell (Wh/kg)	67	89	97
Energy density after charge to 4.0 V/cell (Wh/dm³)	131	187	209
Specific power (10s/50% DOD) (W/kg)	1811	1413	1136
Power density (10s/50% DOD) (W/dm³)	3526	2974	2451
Voltage limits			
Charge (V)	4.0 (4.1 for peak)		
Discharge (V)	2.5 (2.0 for cold cranking)		
Current limits			
Max continuous current (A)	100	250	300
Max peak current during 10s (A)	250	500	500

Fig. 5. VLxP SAFT batteries features.

Equation (29) links $\phi_{ei}(x,t)$ to $c_{ei}(x,t)$. Using linearity assumption H$_3$, if one of these variables is known in the entire cell, and if the second one is known on the positive or negative electrode, equation (29) permits to deduce this second variable on the remaining electrode.

3.2. Model construction

Analytical solution of equation (4) leads to the transfer function that links $c_{si,e} = c_{si}(p, r = R_s)$ to j_i^{Li}, given by:

$$H_{csi}(p, R_s) = H_{csi,e}(p) = \frac{c_{se,i}(p)}{j_i^{Li}(p)}$$

$$= \frac{-R_s}{FD_{si}a_{si}\left(\sqrt{\frac{p}{D_{si}}}R_s \cot h\left(\sqrt{\frac{p}{D_{si}}}R_s\right) - 1\right)}. \quad (30)$$

Due to *coth* function, equation (30) cannot be easily used for simulation or control purpose. A frequency approximation can be

used to overcome this problem. Bode diagrams of $H_{csn,e}(p)$ in Fig. 8 (but a similar one can be obtained for $H_{csp,e}(p)$), indeed show that transfer functions $H_{csi,e}(p)$ can be approximated using the fractional transfer function

$$H_{csi,e}^{app}(p) = \frac{K_{1i}\left(1 + \frac{p}{\omega_{csei}}\right)^{0.5}}{p}. \quad (31)$$

Parameter K_{1i} can be deduced from the Taylor expansion of equation (30). Gain K_{1i} corresponds to the coefficient of the lowest degree term:

$$K_{1i} = \frac{-3}{R_s Fa_{si}}. \quad (32)$$

Then to impose a similar high frequency behavior to equation (30) and to its approximation, a limit study lead to define the corner frequency ω_{csei} by:
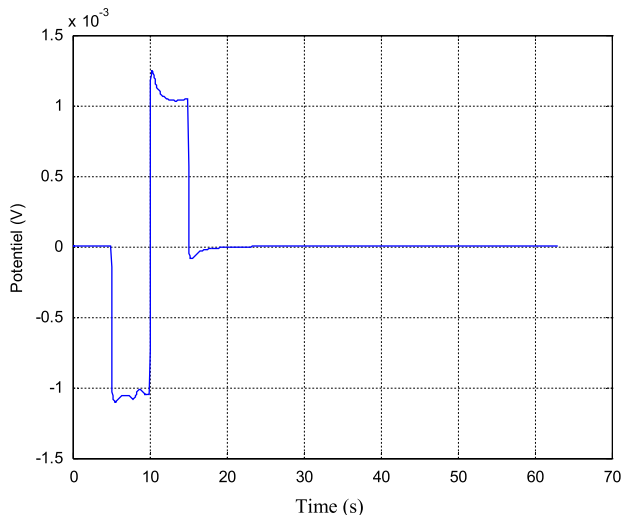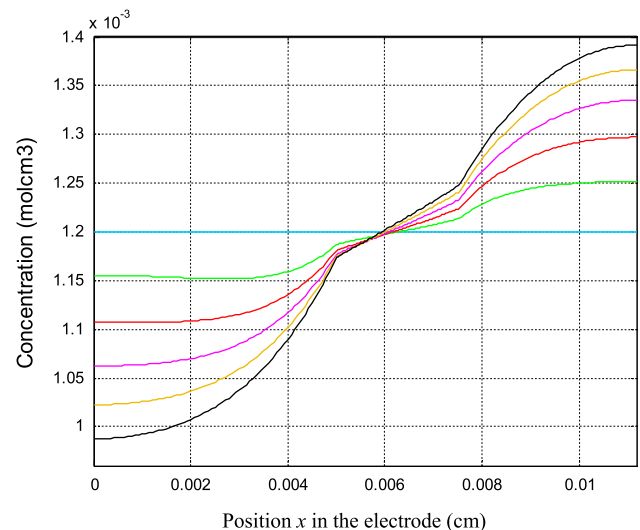

Fig. 6. η_n and η_p overvoltage for the current profile of ±100 A.

Fig. 7. Concentration variation in the electrolyte during the first 10 s.

$$\omega_{csei} = \frac{9D_{si}}{R_s^2}. \tag{33}$$

Fig. 8 validates the approximation of transfer function $H_{csn,e}(p)$ by $H_{csn,e}^{app}(p)$. A similar conclusion can be obtained with transfer function $H_{csp,e}(p)$

Li$^+$ ionic current inside electrolyte is modeled by equation (3) with limit conditions (4). Laplace transform of equation (3) is given by:

$$p\varepsilon_e c_e - \lim_{t \to 0^+} c_e(t,x) = \frac{d}{dx}\left(D_e^{eff}\frac{d}{dx}c_e\right) + \frac{1 - t_+^o}{F}j^{Li}. \tag{34}$$

Solution of this equation is thus:

$$c_e(p,x) = +\frac{(1-t_0^+)}{F}j_{mean}^{Li} + \frac{c_e(0,x)}{p\varepsilon_e} + C_3\exp\left(\frac{\sqrt{p}\varepsilon_e^{0.5(1-p)}}{\sqrt{D_e}}x\right)$$
$$+ C_4\exp\left(-\frac{\sqrt{p}\varepsilon_e^{0.5(1-p)}}{\sqrt{D_e}}x\right), \tag{35}$$

where $c_e(0,x)$ denotes the initial concentration. A cell is made of 3 regions in which concentration variation is thus driven by three equations similar to equation (35). Thus the six constants C_{3n}, C_{3s}, C_{3p}, C_{4n}, C_{4s} and C_{4p} need to be computed using the following limit conditions

$$\begin{cases} c_{en}\left(t, x = \delta^-\right) = c_{es}\left(t, x = \delta^-\right) \\ c_{en}\left(t, x = \delta^- + \delta^{sep}\right) = c_{ep}\left(t, x = \delta^- + \delta^{sep}\right) \\ \left.\frac{\partial c_{en}(t,x)}{\partial x}\right|_{x=0} = 0 \\ \left.\frac{\partial c_{ep}(t,x)}{\partial x}\right|_{x=L} = 0 \\ D_{en}\varepsilon_{en}^p\left.\frac{\partial c_{en}(t,x)}{\partial x}\right|_{x=\delta_n} = D_{es}\varepsilon_{es}^p\left.\frac{\partial c_{es}(t,x)}{\partial x}\right|_{x=\delta_n} \\ D_{es}\varepsilon_{es}^p\left.\frac{\partial c_{es}(t,x)}{\partial x}\right|_{x=\delta_n+\delta_{sep}} = D_{ep}\varepsilon_{ep}^p\left.\frac{\partial c_{ep}(t,x)}{\partial x}\right|_{x=\delta_n+\delta_{sep}} \end{cases} \tag{36}$$

The six constants depends on $J_{i\_mean}^{Li}(t,x)$, and thus due to relations (18) to the current $I(t)$. Transfer functions $H_{esn}(p,x) = c_{en}(p,x)/I(p)$, $H_{ces}(p,x) = c_{es}(p,x)/I(p)$ and $H_{cep}(p,x) = c_{ep}(p,x)/I(p)$ can thus be deduced.

Bode diagrams of $H_{cen}(p)$ in Fig. 9 (but similar ones are obtained for $H_{cep}(p)$) shows that frequency response of this transfer function is similar to those of a first order system. It is thus possible to propose the following approximation:

$$H_{cei}(p) = \frac{K_{cei}}{1 + \frac{p}{\omega_{cei}}}. \tag{37}$$

System identification applied on measures obtained with a 50 A current leads to the following parameters:

$$K_{cen} = 3.7736e^{-7} \text{ mol·cm}^{-3} \text{ and } \omega_{cen}$$
$$= 10^{-0.493445} \text{ rad·s}^{-1};$$

$$K_{cep} = -1.368e^{-6} \text{ mol·cm}^{-3} \text{ and } \omega_{cep} = 10^{-0.862} \text{ rad·s}^{-1}.$$

Contact resistance and also initial solid electrolyte interface can be taken into account by with the resistance R_f in the equation:
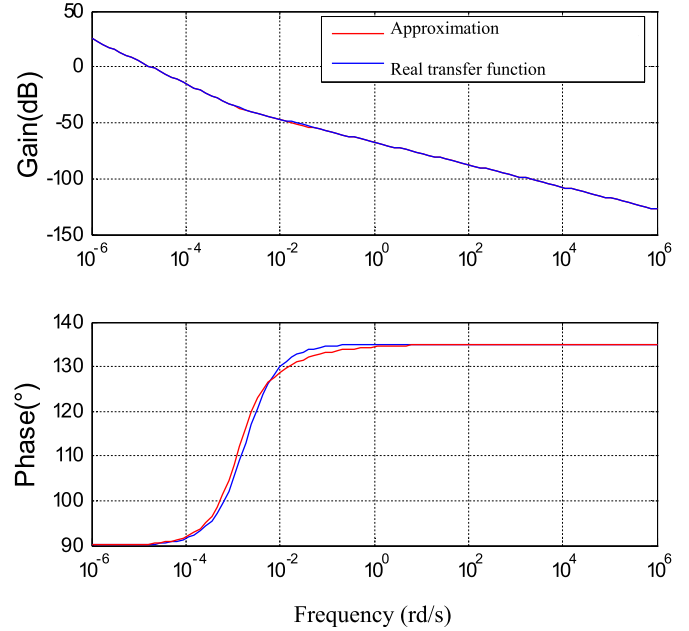

Fig. 8. $H_{csn,e}(p)$ and $H_{csn,e}^{app}(p)$ Bode diagram comparison.

$$U_{batt}(p) = \phi_{sp}(L,t) - \frac{R_f}{A}I(p), \tag{38}$$

Finally, negative and positive electrodes equilibrium potentials are supposed defined by:

$$U_n(x) = 8.00229 + 5.0647z - 12.578z^{1/2} - 8.6322e^{-4}z^{-1}$$
$$+ 2.1765e^{-5}z^{3/2} - 0.46016\exp[15.0(0.06 - z)]$$
$$- 0.55364\exp[-2.4326(z - 0.92)] \tag{39}$$

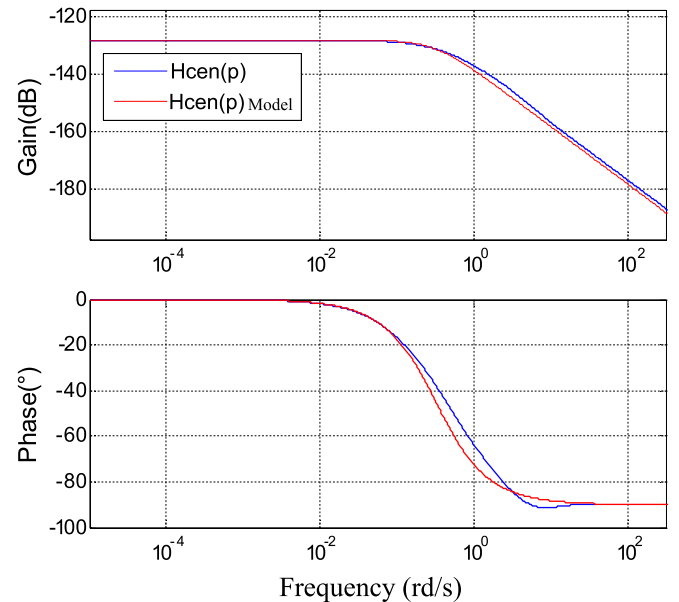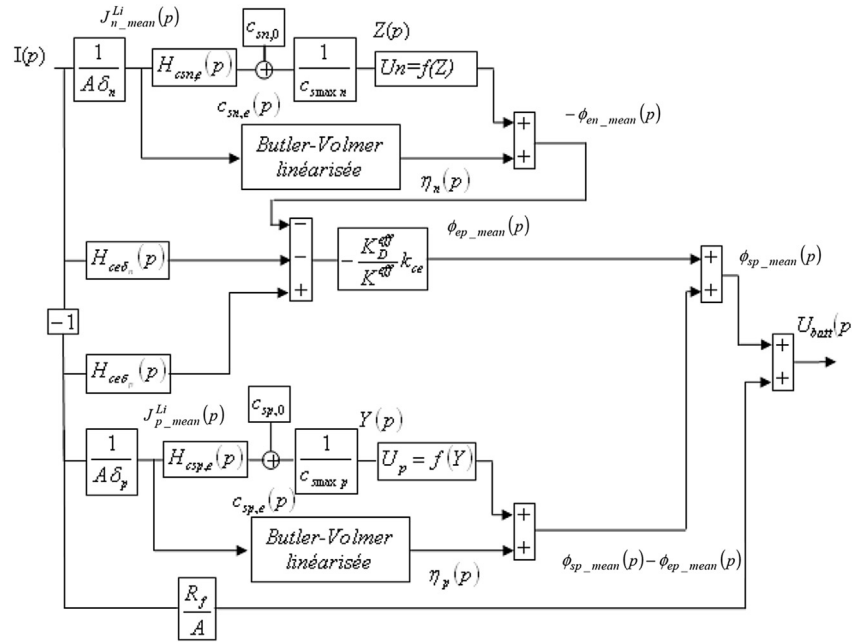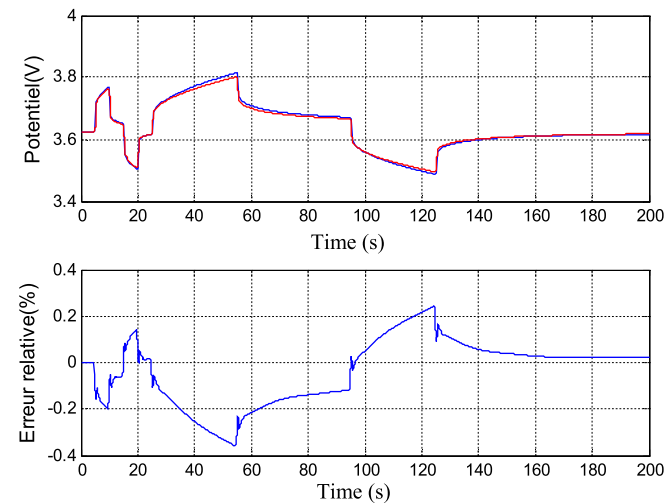**Fig. 9.** Bode diagram of transfer function $H_{cen}(p)$ and its approximation.

Fig. 10. Simplified model obtained.

4. Conclusion and future work

$$U_p(x) = 85.681y^6 - 357.70y^5 + 613.89y^4 - 555.65y^3$$
$$+ 281.06y^2 76.648y - 0.30987 \exp\left(5.657y^{115.0}\right)$$
$$+ 13.1983 \qquad (40)$$

where z and y denote respectively negative and positive electrode solid phase stoichiometries.

Using all the previous comments, a simplified model of a lithium-ion cell can be represented by Fig. 10. A comparison of this model response with a VLxP battery response in Fig. 11 highlights the model accuracy. The errors is always less than 0.4% for a current varying from −100 A to 100 A. This accuracy also validates approximations A_1 and A_2

In this paper a model for lithium-ion batteries has been proposed. This is a fractional model that stems from simplifications of an electrochemical model and is the result of this model partial differential equations solution (solution of diffusion equation (2)). Such an approach permits to get a simple model (low number of parameters in comparison with an approach based on Pade approximation that lead to an integer model with a large number of parameters) in which electrochemical variables and parameters still appear (parameters physical meaning is often lost with an approach based on model reduction). The obtained model permits to simulate the battery voltage with a relative error less than 0.5%. This relative error value has been obtained through several validation tests [13] (not presented here due to the limited number of pages) under various condition (state of charge, temperature, current values and sign).

The interests of such modeling are multiples. Since the physical parameters of the battery (diffusion coefficients, maximum solid-phase concentration, …) are contained in the model parameters (see Fig. 10), system identification can be used to obtain numerical values of these parameters from input-outputs data. These numerical values can be then used to evaluate the battery state of health. Also, some electrochemical variables still appear in the obtained model, such as the solid phase concentration. Using a state observer (or a Kalman filter), such a model can thus be used to evaluate battery state of charge. In future papers, the authors will develop these applications. Also, the authors will present more simple models, obtained using additional simplifying assumptions and will show how these models has been used to estimate state of charge and available power.

These works on lithium-ion modeling and monitoring take place in the open lab "Electronics and Systems for Automotive" combining IMS laboratory and PSA Peugeot Citroën society.

Fig. 11. Model and battery voltage comparison and relative error at $T = -10\ °C$ and Soc = 50%.

References

[1] J. Chatzakis, K. Kalaitzakis, N.C. Voulgaris, S.N. Manias, IEEE Trans. Ind. Electron. 50 (2003) 990—999.

[2] S. Buller, M. Thele, R.W.A.A. De Doncker, E. Karden, IEEE Trans. Ind. Appl. 11 (2005) 742–747.
[3] P. Singh, R. Vinjamuri, X. Wang, D. Reisner, J. Power Sources 162 (2006) 829–836.
[4] G. Sikha, R.E. White, B.N. Popov, J. Electrochem. Soc. (2005) A1682–A1693.
[5] J. Sabatier, M. Aoun, A. Oustaloup, G. Gregoire, F. Ragot, P. Roy, Signal Process. J. 86 (2006) 2645–2657.
[6] N. Bertrand, J. Sabatier, O. Briat, J.M. Vinassa, Commun. Nonlinear Sci. Numer. Simul. 15 (2010) 1327–1337.
[7] J. Sabatier, M. Cugnet, S. Laruelle, S. Grugeon, B. Sahut, A. Oustaloup, J.M. Tarascon, Commun. Nonlinear Sci. Numer. Simul. 15 (2010) 1308–1317.
[8] M. Cugnet, J. Sabatier, S. Laruelle, S. Grugeon, B. Sahut, A. Oustaloup, J.M. Tarascon, IEEE Trans. Ind. Electron. 57 (2010) 909–917.
[9] A.S. Kandler, D.C. Rahn, C. Wang, IEEE Trans. Control Syst. Technol. 18 (2010) 654–663.
[10] A. SmithKandler, Electrochemical Modeling, Estimation and Control of Lithium-ion Batteries, Pennsylvania University, 2006 (PhD thesis).
[11] J. Newman, K.E. Thomas-Alyea, Electrochemical Systems, third ed., Wiley, 2004.
[12] D.R. Baker, M.W. Verbrugge, J. Electrochem. Soc. 160 (2013) A1.
[13] M. Merveillaut, Modélisation non entière et non linéaire d'un accumulateur lithium-ion en vue de la mise en de la mise en œuvre d'observateur pour l'estimation de variables internes (Bordeaux 1 University PhD thesis), 2011.